

2012



RECENT DEVELOPMENTS IN METALLURGY, MATERIALS AND ENVIRONMENT

CHAPTER 12

Effect of Nd:YAG Laser Welding Process Parameters on Al_4C_3 Formation in Advanced Aluminum Graphite Composites

*E. D. Aguilar-Cortes¹, F. J. Garcia-Vazquez¹, J. L. Acevedo-Davila,
F. Cepeda-Rodríguez, M. I. Pech-Canul²*

¹ COMIMSA

² CINVESTAV-SALTILLO

ISBN 978-607-9023-18-8



Materials

CHAPTER 12

Effect of Nd:YAG Laser Welding Process Parameters on Al_4C_3 Formation in Advanced Aluminum Graphite Composites

E. D. Aguilar-Cortes¹, F. J. Garcia-Vazquez¹, J. L. Acevedo-Davila, F. Cepeda-Hernández, M. I. Pech-Canul²

¹COMIMSA, Ciencia y Tecnología 790, Saltillo, Coahuila, México, 25290.

²Cinvestav-Saltillo, Carr. Saltillo-Monterrey km 13, Ramos Arizpe, Coahuila, México, 75100.

Abstract

Aluminum/Graphite composites (Al/C composites) have the advantages of Al (light weight, easy machinability and good heat conduction) in combination with the advantages of C whiskers (High Young's Modulus, small to negative CTE, high tensile strength and high thermal conductivity). However, Metallographic analysis, EDX and microhardness profile revealed that fibers react with molten aluminum to form the detrimental Al_4C_3 phase in the HAZ and fusion zone. In order to gain information about temperature transformation and formation conditions, scanning electron microscopy, and thermochemistry analysis were used. For experiments, were used power density (I), pulse width (t), frequency (F), travel speed (S) and filler material (M) as independent variables. Thereby, was found that the main process variables that influence the formation of Al_4C_3 are pulse duration and welding speed, and that the effect of these variables cannot be explained only by using a thermodynamic model, requiring a subsequent kinetic analysis.

Keywords: Laser welding; Aluminum/Graphite composites; Al_4C_3 .

1. Introduction

Interfacial reaction in Al/C whiskers reinforced composites is a major limiting factor in the development of sound welds. Reactions between the whiskers and the metal during welding can lead to

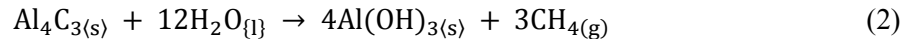
matrix embrittlement, fiber degradation and appearance of interfacial brittle phases. These phenomena produce materials of poor mechanical properties and which are susceptible to corrosion [1].

Several researchers have suggested that the Al_3C and Al_4C_3 carbides produced by various chemical reactions existed in the Al-C system but, further investigations at atmospheric pressure have supported the existence of the Al_4C_3 carbide only [2-7].

Carbon fibers in Al/C composites, are thermodynamically unstable at temperatures above the melting point of aluminum matrix (855K) and reacts with the molten aluminum to form Tetraaluminum Tricarbide, (Al_4C_3) according to the reaction (1), the Al_4C_3 formation is due to the interaction of two main causes, temperatures above the melting point of the matrix and exposure time of the fibers under these temperatures [2-10].



Aluminum carbide crystals are not only brittle, but also highly sensitive to moisture contact and thus promote accelerated fatigue crack growth rates due to their hydrophilic nature. The dissolution of tetraaluminum tricarbide in water or in contact with water vapor (2) decomposes to release methane [2].



The formation of tetraaluminum tricarbide is also due to a higher graphitization of whiskers at extreme temperatures used to reinforce, which causes a more unstable interface. This phase forms by the $L + C \leftrightarrow Al_4C_3$ peritectic reaction at temperatures ranging from 2230 to 2630 K. The phase diagrams of the Al-C system based on the recent experimental results indicate the peritectic equilibrium temperatures of $2253 \pm 293K$ or $2429K$. The second nonvariant equilibrium in the system is the $L \leftrightarrow Al + Al_4C_3$ eutectic equilibrium and in this case, the eutectic is degenerated due to lack of experimental data, Figure 1.

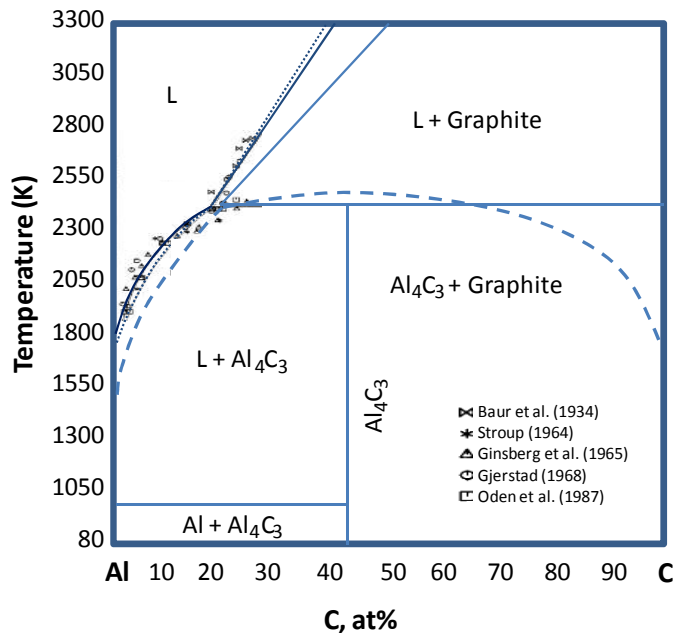


Figure1. Al_4C_3 melts following the peritectic reaction $Al_4C_3 \rightarrow L + Graphite$ at 2330K with the decomposition enthalpy 341.531kJ/mol and entropy 140.371 J/mol*K. Dotted lines indicate metastable continuations of the stable equilibrium

Information about the formation of Al_4C_3 at low temperatures is important; since it would allow us adjust the power density to a minimum value.

The power density is related to the heat input and hence the temperature reached in the fusion zone by the laws of thermodynamics [17], according with:

$$\frac{1}{r} \frac{\partial}{\partial r} \left(\frac{\partial T}{\partial r} \right) + \frac{1}{r} \frac{\partial}{\partial z} \left(kr \frac{\partial T}{\partial z} \right) + Q = \rho C_p \frac{\partial T}{\partial \tau} \quad (3)$$

where r and z refer to radial and axial directions; k , ρ , and C_p respectively refer to thermal conductivity, density, and specific heat of material; T and τ refer to temperature and time variable respectively, and Q depicts internal heat generation per unit time and unit volume

However, the information regarding to the temperature of carbide formation is slight, and therefore, it was necessary to perform an analysis at low temperatures.

2. Thermochemical analysis at low temperatures

The growth of fiber carbide crystals in liquid aluminum may be described as a three-stage process: (i) dissolution of carbon fibers in liquid aluminum; (ii) carbon diffusion, producing a homogeneous distribution in the melt of aluminum and its transport to the growing carbide surface; (iii) deposition of carbon atoms in moving growth steps of the carbide crystal surface [9].

Thus, to reduce or avoid the dissolution and diffusion of carbon is necessary to understand the thermodynamics of this stoichiometric reaction, and that can be defined through its free energy. Due to the lack of information at low temperatures, was made a basic thermochemical analysis, in order to evaluate this experimental part.

First, The Gibbs energy for room temperature is given by:

$$\Delta G_T^\circ = \Delta H_{298}^\circ + \int_{298}^T \Delta C_p^\circ dT - T \Delta S_{298}^\circ - T \int_{298}^T \frac{\Delta C_p^\circ}{T} dT \quad (4)$$

Where,

$$\Delta H_{298}^\circ = -166941.6 \text{ J/mol} \text{ (The heat of formation of } Al_4C_3 \text{) [13]}$$

$$\Delta S_{298}^\circ = -25.008 \text{ J/mol} \cdot \text{K} \text{ (Entropy of formation) [13]}$$

$$\Delta C_p^\circ = 0.069873T + \left(\frac{2635920}{T^2} \right) - 33.388, \text{ J/mol} \cdot \text{K} \text{ (The heat capacity of } Al_4C_3 \text{ reaction)}$$

Reverting to equation (4) for change in free energy with temperature.

$$\Delta G_T^\circ = 33.352T \ln T - 192.37 T - \left(\frac{1.3180 \times 10^6}{T} \right) - 3.4934 \times 10^{-2} T^2 - 1.5126 \times 10^5 \quad (5)$$

But (5), only applicable at temperatures between 298 and 932K, to evaluate the free energy of reaction above this temperature range, we must introduce the free energy of melting of aluminum [13, 14]. The equation for the change in free energy of melting of 4 moles aluminum is:

$$\Delta G_{4Al_{Liq} \leftrightarrow 4Al_{Sol}}^{\circ} = 34.48T \ln T - 177.91 T - 0.02477T^2 - 32392 \quad (6)$$

Where

$$\begin{aligned} \Delta H_{932}^{\circ} &= -43012 \text{ J/mol} \\ \Delta S_{932}^{\circ} &= -46.15 \text{ J/mol} \cdot \text{K} \\ \Delta C_{p4Al_{Liq} \leftrightarrow 4Al_{Sol}}^{\circ} &= 0.04954T - 34.48, \text{ J/mol} \cdot \text{K} \end{aligned}$$

To obtain the free energy of reaction (5) and (6) are added, giving

$$\Delta G_T^{\circ} = 67.832T \ln T - 370.28 T - \left(\frac{1318000}{T} \right) - 5.9704 \times 10^{-2} T^2 - 183650 \quad (7)$$

Now, the new range is reliable up to 1273K.

Figure 2 shows that, temperatures greater than 298K, the minimum Gibbs free energy occurs when all of the Aluminium is in liquid phase. This confirms that the interface Al/C is very unstable and under this premise, any level of power density eliminates carbide formation, because of this, the power density was fixed to the minimum value that allows the fusion of aluminum [15, 16].

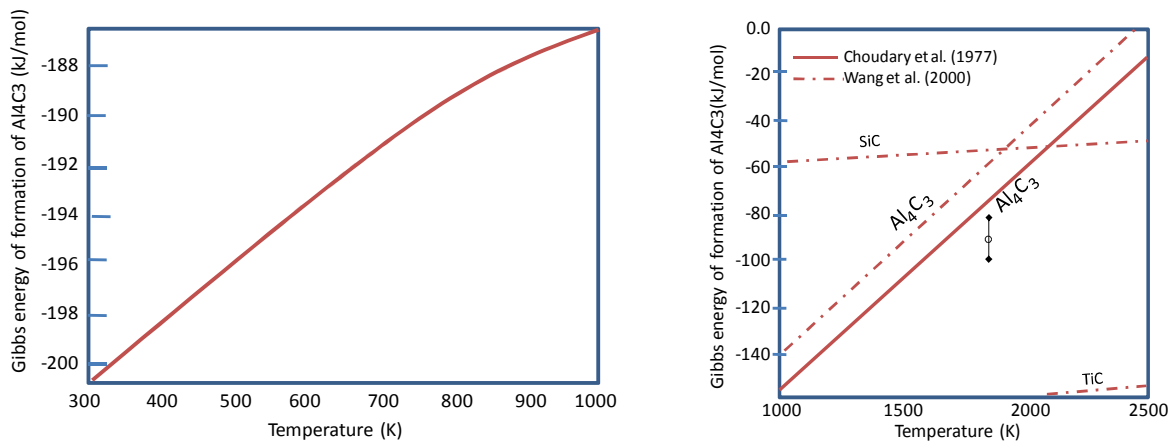


Figure 2. Temperature dependence of the Gibbs energy at low and high temperatures. Dotted lines show the energy of other carbides¹

After finding theoretically that the carbide formation can not be eliminated completely. The next step of this research was to observe the influence of the time parameters (pulse duration and frequency) in the formation of carbide and try to find values that minimize.

¹ Temperature dependence of the Gibbs energy reliable up to 1273K. Verified using Factsage® Software and databases (CINVESTAV, Dr. Martin Pech)

3. Experimental procedures

3.1 Materials

Samples of an Al–Si–Mg casting alloy (A413) reinforced with 0.30 volume fraction of 300 μm average length graphite whiskers were studied. The Al/C composite was produced by Metal Matrix Cast Composites, LLC, by a proprietary molten metal method and then extruded in 216 x 165 x 12.7 mm plates. The chemical composition of the aluminum matrix examined in a JEOL scanning electron microscope (SEM) equipped with EDXS semi quantitative analysis is listed in Table 1.

Al	Sn	Mg	Cu	Mn	Fe	Si	Zn	Ni
BAL.	0.15	0.36	1.0	0.35	2.0	11.0-13.0	0.50	0.50

Table 1. Aluminum matrix chemical composition (wt. %)

Figure 3 depicts the general structure of the composite investigated. The thermal and mechanical properties of Al/C composites are directionally dependent since the graphite whiskers are aligned differently in a xy base plane than in the normal z-direction. These anisotropic properties, in some cases, would restrict the usage of thermal management Al/C composites to one- or two-dimension applications.

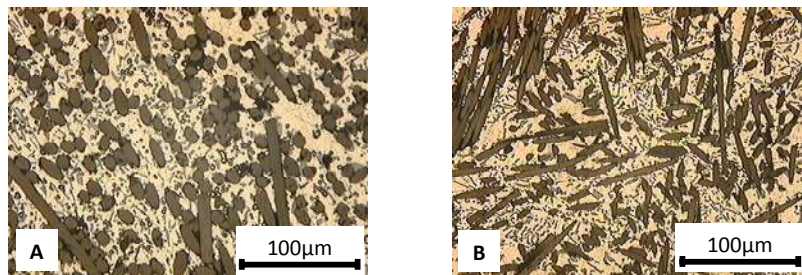


Figure 3. Optical micrographs of the Al/C composite investigated.

- A) Section polished normal to the device mounting surface (through-plane, or “z” section)
- B) Section polished parallel to the device mounting surface (in-plane or “x-y” section)

3.2 Welding procedures and parameters

Laser welding was accomplished by using a BU 160 Nd-YAG laser which is capable of operating at a maximum average output power of 160W. Specimens of 12.7mm X 25.4mm X 3mm dimensions were prepared for bead on plate welding; the surfaces for welding were prepared by fine grinding on 1200 grit size emery paper then ultrasonically cleaned using alcohol. Argon was used as shielding gas and ejected by a backward nozzle inclined at 60° with respect to the laser beam axis. Figure 4 shows the experimental setup for metallographic analysis. In this investigation, 3⁴ full factorial design was used, and Table 3 shows this parameters. Focal length, Argon flow and focus area was fixed for all welds.

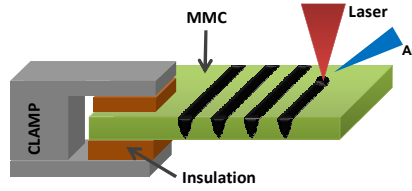


Figure 4. Experimental setup

I (MW/cm ²)	F (Hz)	t (ms)	s (mm/s)	L (mm)	f (L/min)	A (cm ²)
0.95	10	3	1	200	3	0.003
1.00	15	4	3			
1.05	20	5	5			

Table 2. Design of welding experiments. Power density (I); Pulse width (t); Frequency (F); travel speed (s); Focal length (L); Argon flow (f); Focus area (A).

3.3 Scanning electron microscopy

Prior to examination, all specimens were heavily etched with a Keller's solution. These specimens were then examined in a JEOL scanning electron microscope (SEM) equipped with EDXS semi quantitative analysis using an accelerating voltage of 15 kV, spot size of 40 and a working distance of 11 mm. Regions within the fusion zone were examined and the morphology of the major phases present identified.

4. Results and discussion

4.1 Optical Microscopy.

Structural changes in the Al/C composite as a result of Nd:YAG Laser welding are presented in Figures 5 and 6. Figure 5 shows that the fusion zone has three distinct regions. The A region, in the middle of bead, is dominated by an acicular microstructure. In the intermediate region B, the population density of the graphite whiskers is redistributed and a band of voids is present. The D region, nearest to the base material, is defined by a distribution of graphite whiskers particles retained their original clear cut edges without any evidence of interfacial reaction phases.

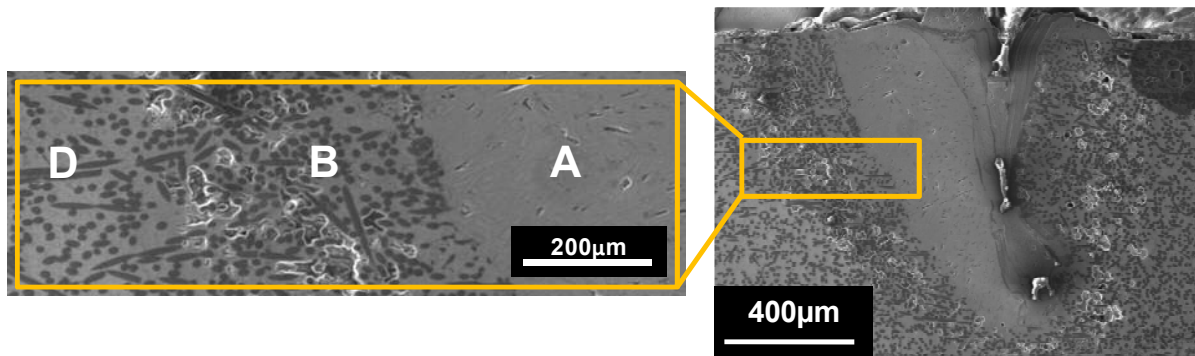


Figure 5. Optical microscopy image of a transverse section in a Nd:YAG weld. Capital letters indicate central (A), fusion (B) and base material (D) regions.

When moving toward the centre of the bead, the composite structure underwent a clear modification with evident redistribution of the graphite whiskers and the corresponding presence of coarse Al_4C_3 needles (Figure 6). Microhardness profiles (Figure 7) taken across the weld bead showed a remarkable increase of hardness with peak values of about 250 HV in the central region (zone A) and this was confirmed by the EDX analysis (Figure 7).

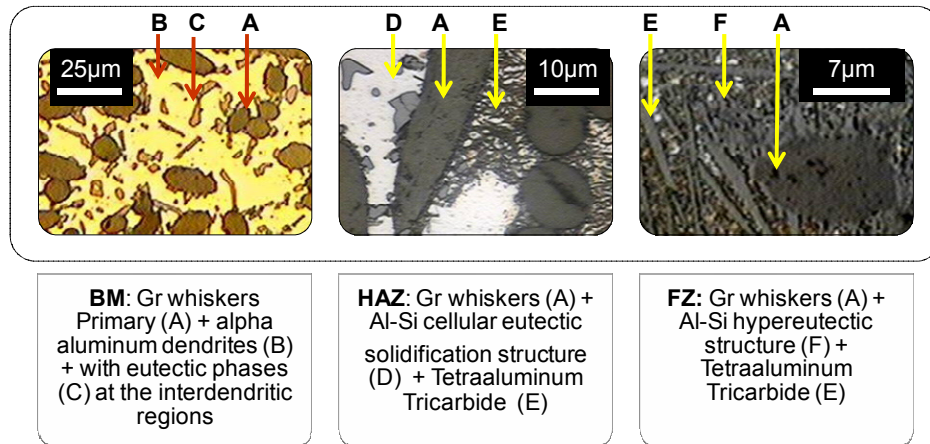


Figure 6. Light micrograph of the base material, heat affected and intermediate fusion zone region in a pulsed Nd:YAG weld.

#	I (MW/cm ²)	t (ms)	s (mm/s)
3	1.4	2,5	0,5
4	1.4	3,5	2,5
12	1.4	3,5	0,5
14	1.4	4,5	1,5
11	1.1	4,5	0,5

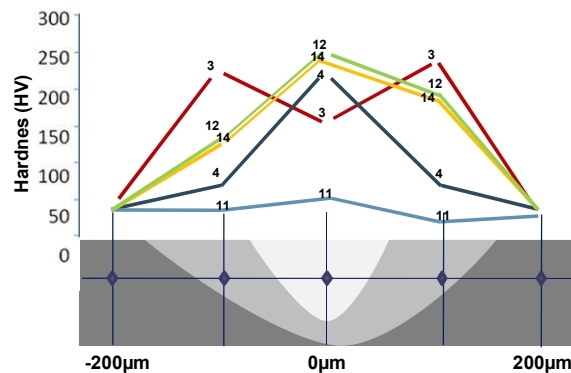


Figure 7. Effect of parameters on microhardness and Al_4C_3 formation. The hardness of the weld joint increases with the quantity of Al_4C_3 . (I) Power density; (t) Pulse width; (s) travel speed.

The microstructure in the center region of the fusion zone is shown in Figure 8. This microstructure is dominated by large Al_4C_3 plates. The coarseness and distribution of Al_4C_3 plates were observed to change as a function of position. Another thing we noticed was that power intensity, pulse width and speed have strong influence on microhardness due to Al_4C_3 formation.

At. %	C	O	Al	Si
Al_4C_3	33.28	5.58	54.36	6.77
Matrix	8.74	3.03	73.74	14.48

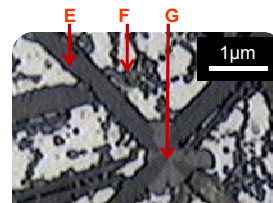


Figure 8. EDS analysis of Al-Si hypereutectic structure (F) + Tetraaluminum Tricarbide (E)+ primary silicon (G) in the center fusion zone region of a pulsed Nd:YAG weld.

4.2 Discussion

During the welding process of aluminium-graphite whiskers reinforced composites, aluminum carbide formation takes place at the interface between the aluminum matrix and the fiber. The presence of carbide needles may strongly influence the mechanical properties of the composite [11]. In this connection, essential information is likely to be obtained by investigating the peculiarities of the carbide formation with the aim of finding possibilities for a procedure-process control.

In a transverse section of a pulsed Nd:YAG weld made in this Al/C composite material, several distinct regions exist within the fusion zone. It was observed by SEM that the nature of these regions is a function of the stability of the graphite whiskers (in liquid aluminum), and basically, this stability is a function of temperature (power density) and contact time (pulse width, frequency and travel speed). This was in agreement with other researchers [12-15]. See Figure 9.

The results indicate that the main welding parameter reduces the amount of carbide is the power density, under this assumption is logical to think that the formation of carbide is stretch linked to the temperature reached in the weld pool. The next step of this study was to find out if there is a minimum temperature of formation (by a thermochemistry analysis) in order to reduce the power density.

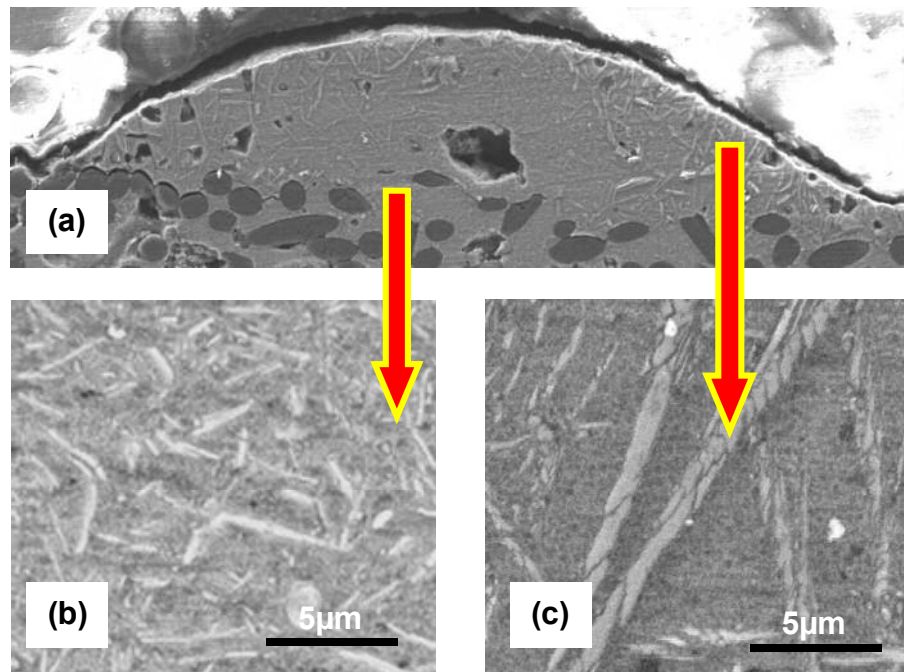


Figure 9. A first observation showed that at low heat input, the dissolution of graphite reinforcement was minimized, and was found only a small region of $Al_4C_3 + Si +$ eutectic cell structure in the middle of fusion zone. (a) General cross section using $I = 1 \text{ MW/cm}^2$, $t = 5\text{ms}$, $F = 20\text{Hz}$, $s=3\text{mm/s}$. (b) Central zone. This solidification structures are identify to as eutectic dendrites with 6% carbon. (c) External zone. Only traces of carbide are present.

And, that the rapid heating and cooling rates possible with minimal energy-density processes make the use of lasers attractive as a technique for welding whisker-reinforced, Al/C composites. In the present work, short pulse lengths and high frequency levels were used to affect rapid weld thermal cycles and low heat input levels to preclude the formation of Al_4C_3 as shown in Figure 10, however, this affirmation requires a kinetic analysis to explain how all of variables affect the formation of carbide.

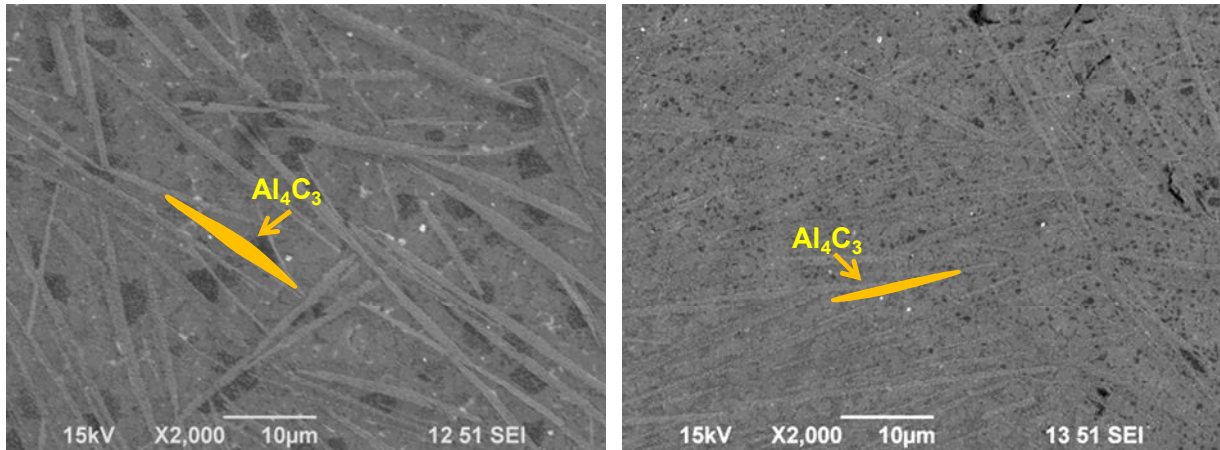


Figure 10. Formation of Al_4C_3 is a function of temperature (power density) and contact time (pulse width and frequency). This was in agreement with other researchers [1-15] a) $t = 8 \text{ ms}$; $I = 1.6 \text{ MW/cm}^2$ b) $t = 4 \text{ ms}$; $I = 1.5 \text{ MW/cm}^2$

5. Conclusions

This research studies effects of laser on Al_4C_3 formation of Al/Graphite composites. We found:

- The hardness of the weld joint increases with the quantity of Al_4C_3
- During the welding of aluminum-graphite composites, aluminum carbide formation takes place at the interface between the aluminum matrix and the fiber, this is a function of temperature (power density) and contact time
- According to thermodynamic analysis, carbide formation begins when the molten aluminum is in contact with graphite and during the weld process of Al-C composites by means of pulsed Nd:YAG laser, carbides will grow predominantly at the time of fiber contact with liquid aluminum but not during matrix solidification and subsequent cooling.
- The growth rate of carbide crystals is limited by the interface kinetics rather than by the thermodynamics. A kinetic analysis allows effective methods of welding process control to be found; for example, growth step retardation by means of shorts welding pulses and high levels of pulse frequency.

Acknowledgements

We would like to thank financial and technical supports from Corporación Mexicana de Investigación en Materiales, MMCC Ltd and the Texas A&M University.

References

1. Mercier, S. "Interfacial reactivity in aluminum/carbon fibre composites", *Journal de Physique IV*, Volume 03, No. C7 (1993), pp 1723-1726.
2. T. Etter, P. Schulz, M. Weber, J. Metz, M. Wimmeler, J.F. Löffler, P.J. Uggowitzer. "Aluminium carbide formation in interpenetrating graphite/aluminium composites", *Materials Science and Engineering*, (2007), pp 1-6.
3. T. Etter, M. Papakyriacoub, P. Schulz, P.J. Uggowitzer. "Physical properties of graphite/aluminium composites produced by gas pressure infiltration method" *Carbon* (2003), pp 1017-1024.
4. D. Steffens, B. Reznik, V. Kruzhanov, W. Dudzinski. "Carbide formation in aluminium-carbon fibre reinforced", *Journal of Materials Science*. Vol. 3 (1997), pp 5413-5417.
5. V. Turkevich, A. Garan, O. Kulik, I. Petrusha, "Phase diagram and diamond synthesis in the aluminum-carbon system at a pressure of 8GPa", en: *Innovative Superhard Materials and Sustainable Coatings for Advanced Manufacturing*, Springer, (2005), pp 334-345.
6. C. Qui, "Solubility of carbon in liquid Al and stability of Al₄C₃" *Journal of Alloys and Compounds*, (1994), pp 55-60.
7. Z. Yunhe, W. Gaohua. "Comparative study on the interface and mechanical properties of T700/Al and M40/Al composites", *Rare Metals*, Vol. 29, No. 1 (2010), pp 102-108.
8. Lu, W. Thermodynamic assessment and experimental investigation of Fe-Al-C system. *Journal of Materials Science and Technology*. (2007), pp 771-774.
9. J. Gröbner, H.L. Lukas, F. Aldinger, J. "Thermodynamic calculations in the Y-Al-C system" *Journal of Alloys and Compounds*. No. 220 (1995). pp 8-14.
10. M. Besterci, L. Parilák. "Microstructure and Mechanical properties of Al-Al₄C₃ materials" *Slovak Academy of Sciences*. (2004)
11. S. Mercier, P. Ehrburger, J. Lahaye. "Interfacial reactivity in aluminum/carbon fibre composites". *Journal de Physique IV*. Vol. 3 (1993). pp 1723-1727.
12. H.M. Wang, Y.L. Chen, L.G. Yu "'In-situ' weld-alloying/laser beam welding of SiCp/6061 Al MMC". *Material Science and Engineering*, (2000). pp 1-6.
13. O. Kubaschewski, (1967). *Metallurgical Thermochemistry* (Fourth edition). Pergamon Press. ISBN 0 08 011887 9, NY USA.
14. M. W. Chase, NIST-JANAF Thermochemical Tables, Fourth Edition. *Journal of Physical and Chemical Reference Data*. (1998), pp 879-901.
15. P. Bassani, "Effect of process parameters on bead properties of A359/SiC MMCs welded by laser". *Composites*. (2007).
16. L. E. Simon, "Laser Welding Equipment and Process Validation". *The University of Wisconsin*. (2009).
17. S. Bag, A. Trivedi, A. De, "Development of a finite element based heat transfer model for conduction mode laser spot welding process using an adaptive volumetric heat source", *International Journal of Thermal Sciences*, (2009), pp 1923-1931.

Para mayor información:

Edgar D. Aguilar Cortes: edgaraguilar@comimsa.com